ChemPubSoc Europe

DOI: 10.1002/cmdc.201700654

CHEMMEDCHEM Communications

SPECIAL ISSUE

Comparative Molecular Dynamics Simulation of Aggregating and Non-Aggregating Inhibitor Solutions: Understanding the Molecular Basis of Promiscuity

Mohammad A. Ghattas,[a] Richard A. Bryce,[b] Sara Al Rawashdah,[a] Noor Atatreh,[a] and Waleed A. Zalloum*[c]

The presence of false positives in enzyme inhibition assays is a common problem in early drug discovery, especially for compounds that form colloid aggregates in solution. The molecular basis of these aggregates could not be thoroughly explored because of their transient stability. In this study we conducted comparative molecular dynamics (MD) simulations of miconazole, a strong aggregator, and fluconazole, a known non-aggregator. Interestingly, miconazole displays full aggregation within only 50 ns, whilst fluconazole shows no aggregation over the 500 ns simulation. The simulations indicate that the center of the aggregate is densely packed by the hydrophobic groups of miconazole, whereas polar and nonpolar groups comprise the surface to form a micelle-like colloid. The amphiphilic moment and planar nature of the miconazole structure appear to promote its aggregating behavior. The simulations also predict rapid aggregate formation for a second known promiscuous inhibitor, nicardipine. Thus, MD appears to be a useful tool to characterize aggregate-prone inhibitors at molecular-level detail and has the potential to provide useful information for drug discovery and formulation design.

Promiscuous inhibitors are defined by Shoichet et al.[1] as organic molecules that form colloidal aggregates in solution and nonspecifically inhibit various enzymes. Previous evidence indicates that these aggregators produce their effect by adsorbing enzyme molecules on their surface, sequestering them and then promoting protein unfolding.[2,3] It has been noted that 95% of the artefactual hits obtained in enzyme testing are based on colloidal aggregation followed by enzyme sequestering, whereas only 5% of false positives can be attributed to all other unspecific inhibition mechanisms, such as oxidation, assay interference, and covalent modification.[4]

There are several common characteristics of promiscuous inhibitors, such as noncompetitive inhibition, a weak relationship between structure and activity, time-dependent inhibition, poor specificity, and formation of particles within the nanometer diameter range.[4–6] There are several methods to eliminate or attenuate the promiscuous activity of these aggregators. Approaches include the use of dynamic light scattering to reveal aggregation, centrifugation of the inhibitor stock solution before testing, removing the pre-incubation step in enzyme assays, and more efficiently adding detergent to the testing solution (e.g., Tween-80).[7–10] Furthermore, aggregation behavior can be predicted by computational tools prior to virtual or high-throughput screening.[7,11–13]

Compound aggregation not only affects enzymes but has also been shown to interfere with: G protein-coupled receptors by artefactual antagonism,[8] cell-based assays by inhibiting drug penetration through the membrane,[14] and multiple in vivo processes such as absorption and distribution of drugs.[15] Interestingly, such aggregates show some ability to inhibit amyloid formation, purportedly via a sequestering-based mechanism.[16] Furthermore, the colloidal properties of small-molecule aggregators have also demonstrated potential for exploitation in the formulation field, for example, acting as stable vehicles to preserve protein activity,[17] and as nanoparticle formulations for targeted drug delivery.[18] Hence, characterizing the aggregation behavior of these systems at the atomic level provides a basis for developing their colloidal properties for new applications, or alternatively designing out aggregation behavior in order to decrease false hits during early-stage drug discovery.

Investigations of the molecular mechanism of aggregation can be started by comparing the structures of a known aggregator (miconazole) with a known non-aggregator (fluconazole), especially if these compounds belong to the same structural family (Table 1). Despite this, these two compounds have substantial differences in physicochemical properties: for instance, fluconazole is smaller, less hydrophobic, and has greater polar surface area than miconazole. This difference in polarity can explain, to some extent, why fluconazole does not aggregate whilst miconazole does, as low water solubility has been shown to be a strong factor favoring aggregation.[19] However, many insoluble compounds have previously been shown not to be promiscuous inhibitors.[7] Thus, there are other factors

[a] Dr. M. A. Ghattas, S. Al Rawashdah, Dr. N. Atatreh
College of Pharmacy, Al Ain University of Science and Technology, Al Ain, 64141 (UAE)

[b] Dr. R. A. Bryce
Division of Pharmacy and Optometry, School of Health Sciences, Faculty of Biology, Medicine and Health, University of Manchester, Manchester Academic Health Science Centre, Oxford Road, Manchester M13 9PL (UK)

[c] Dr. W. A. Zalloum
Faculty of Health Sciences, American University of Madaba, Amman (Jordan)
E-mail: w.zalloum@aum.edu.jo

Supporting information and the ORCID identification number(s) for the author(s) of this article can be found under: https://doi.org/10.1002/cmdc.201700654.

SPECIAL ISSUE This article is part of a Special Issue on Cheminformatics in Drug Discovery. To view the complete issue, visit: http://onlinelibrary.wiley.com/doi/10.1002/cmdc.v13.6/issuetoc.

Table 1. Structures of miconazole and fluconazole and their selected physicochemical properties.

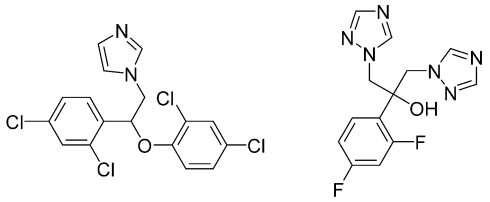

Property	Miconazole Aggregator	Fluconazole Non-aggregator
M_r [Da]	416.1	306.3
log $P_{(o/w)}$	6.1	−1.1
ASA[a]	542.4	476.3
TPSA[b]	27.0	81.7
FASA_H[c]	0.907	0.681
FASA_P[d]	0.093	0.319
Surf_A[e]	5.18	1.96

[a] Water-accessible surface area. [b] Topological polar surface area. [c] Fractional hydrophobic ASA. [d] Fractional polar ASA. [e] Amphiphilic moment.

that promote aggregation, causing two compounds belonging to the same family to behave differently in the assay solution. Colloid aggregators have been difficult to study at the molecular level because of their polydispersity and transient stability.[20] Therefore, computational methods, in particular molecular dynamics (MD) simulations, appear well placed to provide this level of detail for these systems.

Computational tools for aggregation prediction are able to rapidly detect true positives; however, they are prone to predicting false negatives.[12] We have screened miconazole and fluconazole through the recently developed software tool, Aggregator Advisor.[12] Although miconazole and nicardipine were correctly predicted as aggregators, fluconazole was incorrectly labeled as an "aggregator" or "similar to previously identified aggregator". Hence, in addition to our goal to understand the molecular aspects behind miconazole aggregation, we also examine the ability of the MD simulations to distinguish between the known aggregator and non-aggregator.

Herein we report MD simulations of 500 ns for a known aggregator, miconazole, in order to investigate how such a compound can act as a strong promiscuous inhibitor in multiple enzyme assays. The known non-aggregator, fluconazole, very similar to miconazole in terms of structure, was also simulated, as a negative control. Both miconazole and fluconazole systems were created to mimic the experimental assay conditions, i.e., dissolution in DMSO and water with a given salt concentration (Table S1, Supporting Information).[11] The DMSO concentration in water was set up as 5% (*v*/*v*) as per the reference work,[11] which may not be typical in other types of assay. The system was built with solvation of the solute molecules by DMSO, water and NaCl. Only solvent molecules were allowed to relax initially by conducting energy minimization which was followed by energy minimization for the whole system, including the solute molecules. The system was heated under NVT conditions for 20 ps, and then solvent molecules were allowed to mix for 1.5 ns whilst solute molecules were kept restrained. Both the fluconazole and miconazole systems equilibrated in a short time period, with good mixing of DMSO and water to give a homogeneous mixture (Table S2). Production MD simulations were then carried out for 500 ns under NPT conditions without applying any restraints on the solute molecules (detailed MD simulation protocols are provided in the Supporting Information).

Interestingly, and in line with experimental results,[11] miconazole underwent spontaneous aggregation in a short time period (Figure 1 A); after only 10 ns, all but two of the miconazole molecules combined to form a single aggregate. By 100 ns, all miconazole molecules clustered together to form a single aggregate that remained intact throughout the remaining simulation. In contrast, small transient aggregates of 2–3 fluconazole molecules were observed in the first 10 ns of the MD simulation. However, these trial aggregates failed to grow, and by 50 ns, all drug molecules were individually dispersed throughout the system (Figure 1 B). The rapid discrimination of the experimentally known aggregator from non-aggregator during the MD simulation is striking.

To probe the structural features of this divergent behavior of miconazole and fluconazole, we analyzed their physicochemical properties as a function of time. First, we examined their total solvent-accessible surface area (ASA), fractional polar (FASA_P), and hydrophobic surface area (FASA_H). As expected, aggregate formation decreases the total surface area exposed to solvent for miconazole (Figure 2): ASA decreases rapidly by more than half, from 6244 Å^2 to 3000 Å^2 within 50 ns. On the other hand, the fluconazole molecules experience a temporary drop in their ASA from 5000 Å^2 to 4000 Å^2 which is quickly reversed, indicating initial unstable aggregate formation that rapidly dissolves back into solution after 20–30 ns.

The FASA_H of fluconazole does not change throughout the MD simulations, as the molecules remained dispersed (Figure 2). However, the miconazole solutes exhibit a large change in surface area. The exposed surface area of miconazole becomes less hydrophobic as the FASA_H value decreases from 0.85 to 0.78 (Figure 2 top). This burial of hydrophobic surface area of miconazole is correspondingly accompanied by an increase in polar surface area at the aggregate exterior, with FASA_P increasing from 0.15 to 0.22 (Figure S1). Therefore, although as an individual hydrophobic molecule miconazole seems to be incapable of dissolving into solution, this inability decreases by aggregating with other miconazole molecules to attain greater surface polarity.

The aggregation process of miconazole can also be characterized by its radius of gyration (R_g), globularity and rugosity. By 50 ns, the R_g value stabilizes as smaller aggregates agglomerate to form a single stable aggregate with an average R_g of 9.1 Å (Figure 3). By this point, the aggregate has adopted a spherical and regular shape, with high globularity and low rugosity, respectively (Figure 3); this aggregate remains intact for the rest of the 500 ns simulation. Thus, the size of the aggregate simulated here is ≈1 nm. Experimentally such aggregates are observed in the size range of 30–400 nm.[2] However the simulations appear able to capture the initial stages of ag-

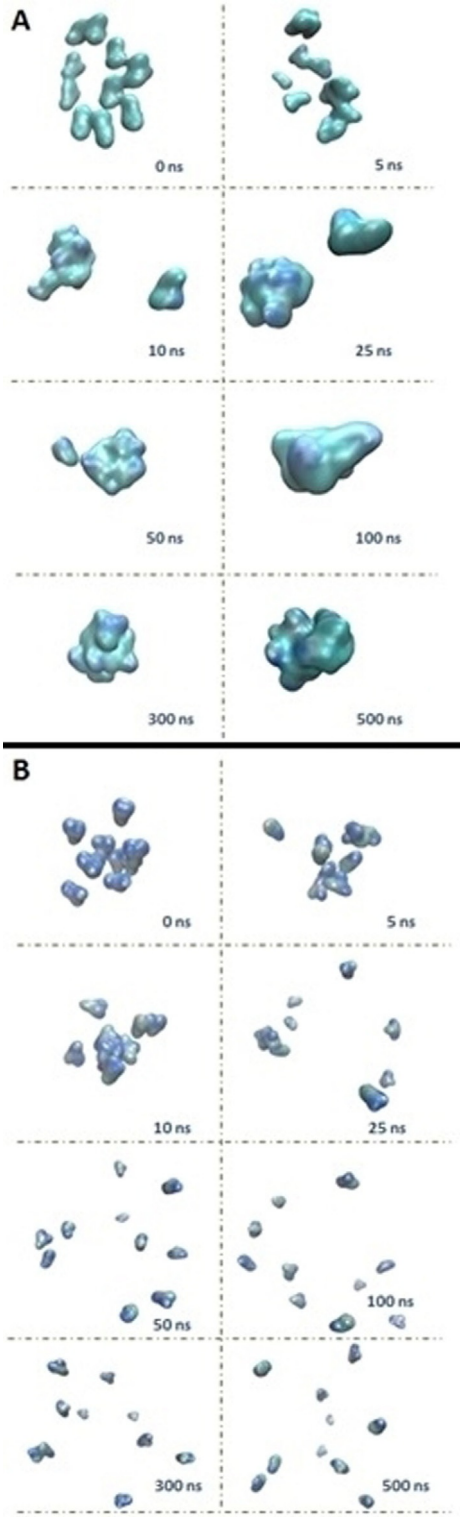

Figure 1. Snapshots of the production MD simulations of A) miconazole and B) fluconazole at 0, 5, 10, 25, 50, 100, 300, and 500 ns. Solute molecules are shown in surface (carbon in green, nitrogen in blue). Solvent molecules and others are omitted for clarity.

gregation, indicating micozanole's predisposition to self-associate. We now consider in greater detail the structural nature of this aggregate.

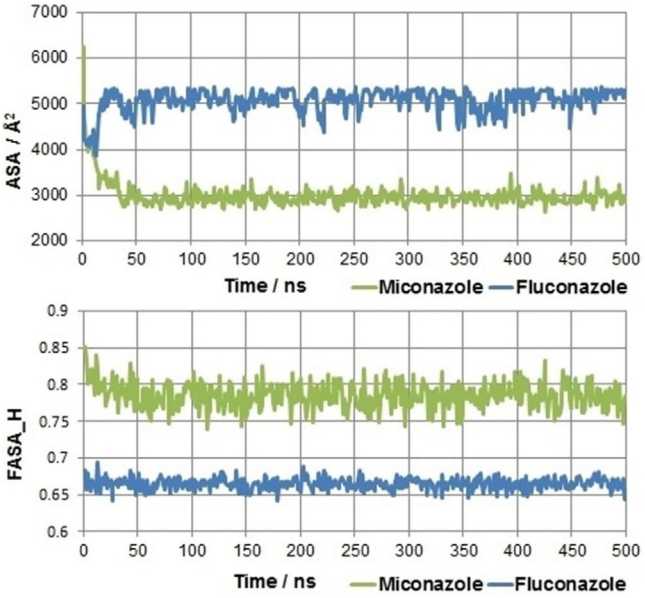

Figure 2. ASA (top) and FASA_H (bottom) calculated for miconazole and fluconazole during the MD simulations.

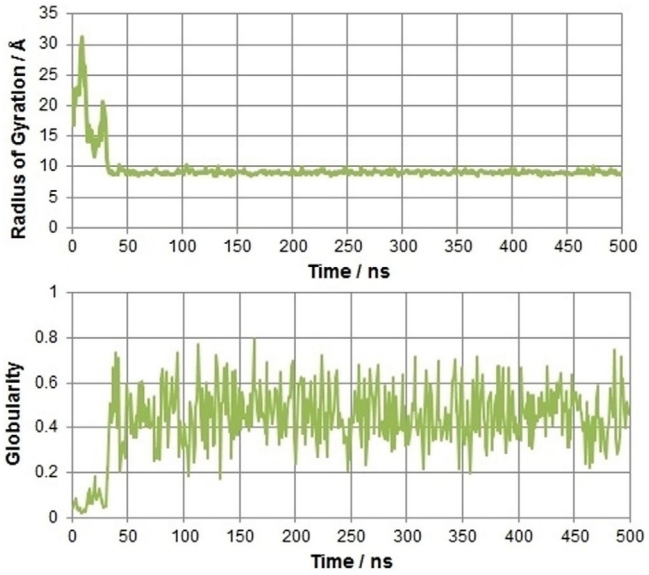

Figure 3. Radius of gyration (top) and globularity (bottom) calculated for miconazole molecules during the whole production MD simulations.

Examination of hydrogen bonding between miconazole and solvent finds an average of 11 hydrogen bonds formed. This number remains almost the same over the entire simulation, further indicating that polar groups remained exposed to solvent and are not sequestered (Figure S2). With its greater number of groups capable of hydrogen bonding (Table 1), fluconazole makes three times more hydrogen bonds with water than miconazole, with an average of 34 hydrogen bonds (Figure S2). This explains why the fluconazole molecules completely dissolve in the system and do not form a stable aggregate; indeed, previous experimental results indicate that compounds with good water solubility ($\log S > -5$) tend less to become ag-

gregators.[19] We note that DMSO seems to play no influential role in the aggregation process of miconazole or in the solubilization process of fluconazole, as both solutes were involved in minimal hydrogen bonding with DMSO (Figure S2).

For further insight into the structural features of the miconazole aggregate, we performed a cluster analysis of the trajectory based on solute heavy-atom RMSD (see the Supporting Information for methodological details). The top five clusters comprise 40% of the analyzed MD trajectories, where the top-ranked cluster includes the highest fraction of 10% compared to the other four clusters (Table S2). The average distance between members in a given cluster is similar for all clusters, which is ~9 Å. The average distance of the cluster to every other cluster is almost the same for the top five clusters (≈14.5 Å), as shown in Table S2.

The centroid of the top miconazole cluster (Figure 4) indicates that the solute molecules pack well into a single aggregate; centroid configurations for the other four clusters are shown in Figure S6. This agrees with the suggestion that, experimentally, miconazole and other strong aggregate formers are densely packed into filled, not hollow, spheres.[21,22] As implied by the analysis of solvent-accessible surface area above (Figure 2), the hydrophobic miconazole dichlorophenyl groups concentrate in the center of the aggregate; conversely, the polar imidazole groups and other non-polar functionalities combine together at the surface; overall a micelle-like sphere is formed in solution (Figure 4), consistent with previous experimental results that the aggregator colloids resemble micelle behavior.[21] The micelle-like colloid property of miconazole can be correlated to its high amphiphilic moment (Surf_A = 5.18), relative to a lower value for fluconazole (Surf_A = 1.96), which allows it to emulate the aggregation behavior of surfactant molecules in solution to form a micelle.

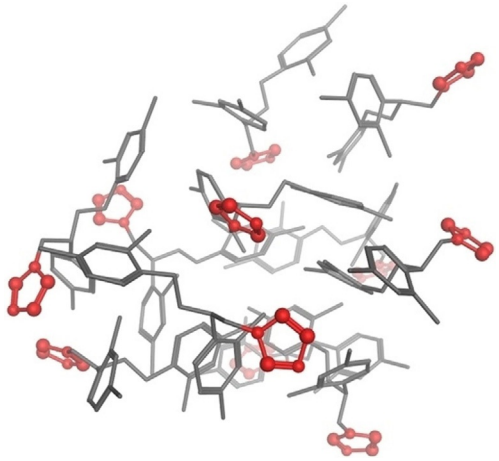

Figure 4. The configuration of miconazole molecules found in the centroid frame of cluster 1. Imidazole rings are shown in ball-and-stick format in red, and the rest of the molecules are shown as gray sticks.

For more detail of the types of interactions present in the miconazole aggregate, the top five clusters were quantitatively analyzed in terms of hydrogen bonding, halogen bonding, van der Waals contacts, stacking interactions, and cation–arene interactions (Table 2). Nonspecific van der Waals contacts are the prevalent interaction in the aggregate; π–π stacking interactions also appear significant, with an average of eight interactions per aggregate (Table 2), i.e., 73% of the miconazole molecules are involved in a π–π stacking interaction. This agrees with a previous observation that aggregate formers are usually extensively conjugated.[11] Arene systems seem not only to be involved in stacking interactions but also in cation–arene interactions, but to a lesser extent, with an average of one interaction per aggregate (Table 2). Finally, hydrogen bonding seems to play no role in miconazole–miconazole interactions, only possible via the protonated form of the imidazole group; but it does play a role in the formation of micelle-like colloid through solvent interactions. In summary, van der Waals contacts and π-stacking interactions seem to be the main driving forces for aggregate formation.

Table 2. Average numbers for various types of interaction based on 10% of the total frames in each cluster of miconazole and nicardipine.

# Cluster	Hydrogen bond	Halogen bond	vdW[a]	Stacking interactions	Cation–arene
Miconazole					
1	0.2	0.0	2484.3	8.7	1.2
2	0.0	0.0	2459.5	8.1	1.0
3	0.0	0.0	2450.7	8.0	0.9
4	0.0	0.1	2444.5	6.2	1.0
5	0.0	0.1	2468.6	8.1	0.6
Nicardipine					
1	1.6	0.0	3191	13.4	11.3

[a] van der Waals contacts.

Perhaps the most striking feature of these simulations is the rapidity with which the MD simulation observes miconazole aggregation, in contrast to the persistent non-aggregation of fluconazole on the same time scale. We were therefore interested to examine if this aggregation behavior extends beyond miconazole. We ran an indicative simulation of another known aggregator, nicardipine. This compound is larger and more polar than miconazole, with a FASA_P value of 0.213 (Table S4). We simulated 11 molecules of nicardipine in DMSO/water solution for a shorter time of 155 ns. Even for this briefer simulation, it was evident that nicardipine has a strong propensity to aggregate, with nicardipine molecules starting to cohere early in the MD simulation (Figure 5); two large aggregates had formed by 50 ns. From this point, one aggregate grows in size while the other begins to dissolve. At 98 ns, a single aggregate of nine of the 11 nicardipine molecules is formed and remains intact to the end of the 155 ns.

Nicardipine showed aggregation behavior similar to that of miconazole, especially in that it exhibited a large decrease in its solvent-accessible surface area at ~50 ns (Figure 6). The aggregate formed has an R_g value of ~10 Å (Figure S3), similar to the value for miconazole aggregate. In contrast to miconazole, the aggregate of nicardipine displayed a lesser spherical shape, with a globularity factor equilibrated at only 0.22 (Figure 6); this rough shape is clearly observed for the final

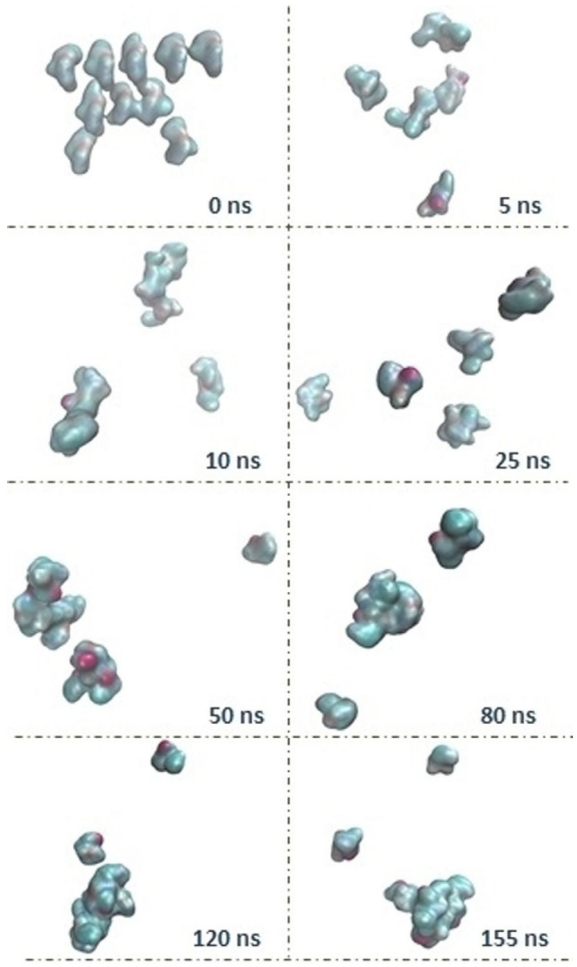

Figure 5. Snapshots of the production MD simulations nicardipine at 0, 5, 10, 25, 50, 80, 120, and 155 ns. Solute molecules are shown in surface (carbon in green, nitrogen in blue). Solvent molecules and others are omitted for clarity.

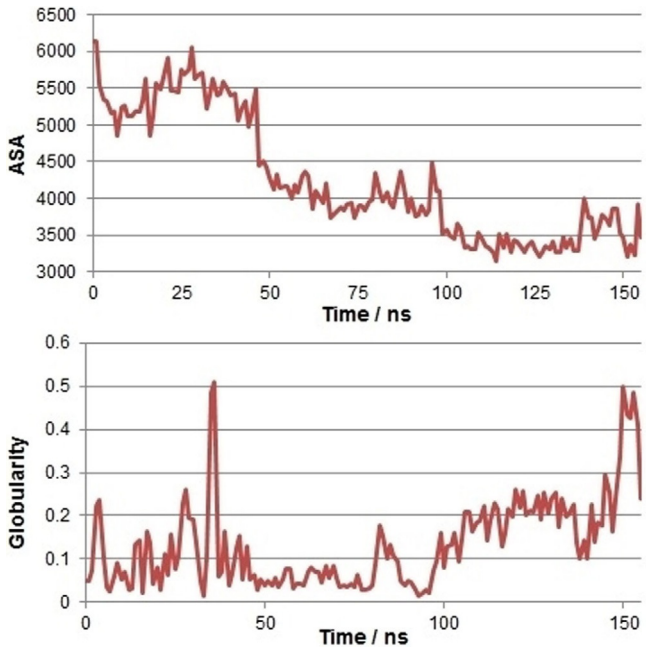

Figure 6. ASA (top) and globularity (bottom) calculated for the nine aggregating nicardipine molecules during the MD simulations.

snapshot. Another major difference with miconazole is that nicardipine showed no change in FASA_P and FASA_H throughout the simulation (Figure S4). Nicardipine has a five-fold larger surface area (TPSA = 114) than miconazole (TPSA = 27), which means that there are multiple polar spots on the nicardipine structure that cannot be all accommodated on the exterior of the aggregate. Hence, nicardipine forms a less micelle-like colloid in solution relative to miconazole, which correlates with the weak amphiphilic moment of nicardipine (Surf_A = 2.7) in comparison with miconazole (Surf_A = 5.18, Table S4).

Nicardipine configurations were clustered. Interestingly, the top-ranked cluster comprised 30% of the total number of the analyzed frames (Table S5). The polar groups of nicardipine can be seen in both the outer surface of the aggregate and, to lesser extent, in the center of the aggregate where they form hydrogen bonds with each other (Figure S7). Similar to miconazole, van der Waals contacts, along with the two stacking interaction types (i.e., π–π and arene–π) have the largest influence on nicardipine aggregation (Table 2). We note that arene–π interactions have a greater influence on the cohesion of the nicardipine molecules than miconazole, probably due to the greater basicity possessed by the former compound. To sum up, van der Waals contacts and stacking interactions seem to be the main driving forces for aggregate formation for both miconazole and nicardipine; this is due to a number of hydrophobic and aromatic groups.

In this study, we have investigated the molecular features of the aggregation-based inhibitor miconazole in solution, compared with the non-aggregator fluconazole, via 500 ns molecular simulations in water/DMSO solution. We found that fluconazole showed no aggregation at all throughout the 500 ns simulation. By contrast, full miconazole aggregation was complete after only 50 ns and remained stable during the rest of the simulation. The aggregate formed a micelle-like sphere that sequestered hydrophobic dichlorophenyl groups exposed mainly polar (imidazolyl) groups on the surface. Experimentally, miconazole colloids have been shown to adsorb enzyme molecules, unfold them, and to cause the undesired promiscuous inhibition effect.[3] The most populated configurations of the miconazole aggregate indicate a densely packed particle, in line with published data. Interestingly, our MD simulations of another known aggregator, nicardipine, also indicated rapid aggregation on the simulation timescale ($\approx$50 ns). We found that the composition of the micelle formed by miconazole differs from nicardipine; in the latter, polar groups are observed both inside and on the surface of the aggregate. This variation in the aggregation behavior was related to the large difference in amphiphilic moment for miconazole and nicardipine. On the other hand, the van der Waals contacts and stacking interactions were observed to be the main driving force for aggregate formation, reflecting the correlation between hydrophobicity/aromaticity and aggregation.

As noted above, these simulations are capable of capturing only the initial stages of colloid aggregation. Nevertheless, it is tempting to suggest that such MD simulations could offer a general filter to discriminate aggregators from non-aggregators in medicinal chemistry programs. Clearly, MD is considera-

bly more computationally intensive than rapid 1D/2D property filters, but such simulations could present an accurate first-principles approach for key inhibitor scaffolds of interest.

To provide an initial test of MD simulation to identify aggregators prospectively, we selected ten compounds not yet tested for aggregation and which are challenging in terms of property and similarity space for aggregation prediction filters. These compounds were selected from the US National Cancer Institute ligand library on the basis of their intermediate similarity with known aggregators and intermediate hydrophobicity (see Supporting Information for details). All compounds were prepared in a water/DMSO system, and then MD simulations were conducted for 50 ns. Consequently, the final 10 ns of the simulation were examined for aggregation (Figure 7). Among the ten simulated compounds, eight were predicted as aggregators (Table 3), while only one was predicted as a non-aggregator, compound 187790. Compound 195942 was identified as a partial aggregator, as only 50% of the molecules associated, whereas the rest were dispersed in the solvent. Given these in silico predictions for the ten challenging compounds, it would be of interest to subsequently test these molecules experimentally aggregation.

In summary, promiscuous inhibitor aggregation behavior has been characterized with molecular level detail via MD simulations; this approach has the potential to provide useful guidance in drug discovery and formulation design.

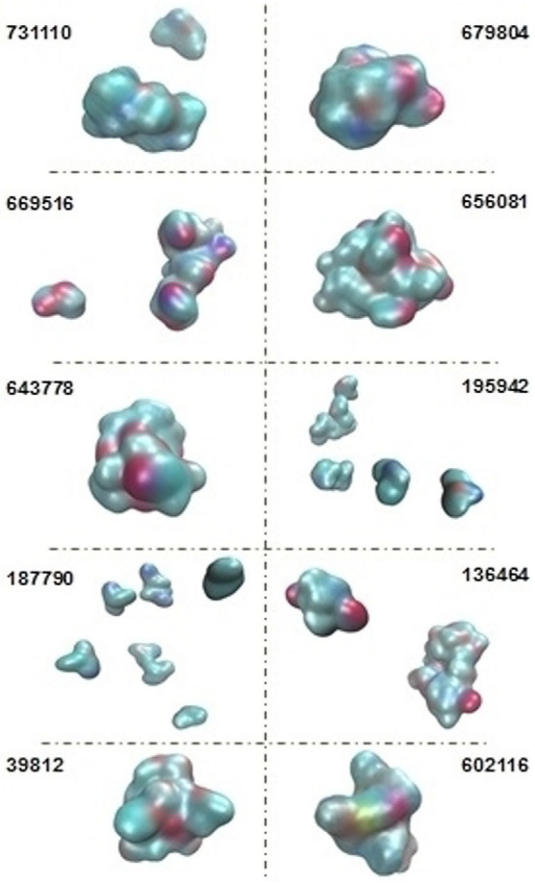

Figure 7. Configuration of miconazole- and nicardipine-like compounds found in the centroid frame of the top cluster from the final 10 ns of simulation.

Table 3. Miconazole- and nicardipine-like compounds along with their aggregate prediction observed in a 50 ns MD simulation.

NCI code	Log $P_{(o/w)}$	# Aggregating molecules (total)	Aggregate prediction[a]
731110	3.81	6 (8)	Aggregate
187790	3.69	2 (8)	Non-aggregate
195942	4.09	4 (8)	Partial aggregate
39812	3.16	8 (8)	Aggregate
656081	3.36	9 (9)	Aggregate
643778	3.44	8 (8)	Aggregate
602116	3.24	8 (8)	Aggregate
679804	3.05	8 (8)	Aggregate
136464	3.29	7 (9)	Aggregate
669513	2.96	7 (9)	Aggregate

[a] Non-aggregator: $<40\%$ of molecules aggregating; Partial aggregator: 40–75% of molecules aggregating; Aggregator: $>75\%$ of molecules aggregating.

Abbreviations

MD: molecular dynamics, ASA: water-accessible surface area, FASA_P: fractional polar ASA, FASA_H: fractional hydrophobic ASA, Surf_A: amphiphilic moment, TPSA: topological polar surface area.

Acknowledgements

We thank Irfan Alibay for assistance with some calculations.

Conflict of interest

The authors declare no conflict of interest.

Keywords: aggregators · colloids · micelles · molecular dynamics · promiscuous inhibitors

[1] B. Y. Feng, B. K. Shoichet, *Nat. Protoc.* **2006**, *1*, 550 – 553.
[2] S. L. McGovern, E. Caselli, N. Grigorieff, B. K. Shoichet, *J. Med. Chem.* **2002**, *45*, 1712 – 1722.
[3] K. E. D. Coan, D. A. Maltby, A. L. Burlingame, B. K. Shoichet, *J. Med. Chem.* **2009**, *52*, 2067 – 2075.
[4] B. Y. Feng, A. Simeonov, A. Jadhav, K. Babaoglu, J. Inglese, B. K. Shoichet, C. P. Austin, *J. Med. Chem.* **2007**, *50*, 2385 – 2390.
[5] L. Yichin, H. B. Maureen, J. Adam, M. Robert, S. Kinjalkumar, C. Kevin, S. Stephen, L. Cristina, L. Marya, O. E. Linda, G. Amy, E. H. Christopher, *J. Biomol. Screening* **2012**, *17*, 225 – 236.
[6] S. L. McGovern, B. T. Helfand, B. Feng, B. K. Shoichet, *J. Med. Chem.* **2003**, *46*, 4265 – 4272.
[7] B. Y. Feng, A. Shelat, T. N. Doman, R. K. Guy, B. K. Shoichet, *Nat. Chem. Biol.* **2005**, *1*, 146 – 148.
[8] M. F. Sassano, A. K. Doak, B. L. Roth, B. K. Shoichet, *J. Med. Chem.* **2013**, *56*, 2406 – 2414.
[9] A. Jadhav, R. S. Ferreira, C. Klumpp, B. T. Mott, C. P. Austin, J. Inglese, C. J. Thomas, D. J. Maloney, B. K. Shoichet, A. Simeonov, *J. Med. Chem.* **2010**, *53*, 37 – 51.
[10] A. J. Ryan, N. M. Gray, P. N. Lowe, C.-w. Chung, *J. Med. Chem.* **2003**, *46*, 3448 – 3451.

[11] J. Seidler, S. L. McGovern, T. N. Doman, B. K. Shoichet, *J. Med. Chem.* **2003**, *46*, 4477 – 4486.
[12] J. J. Irwin, D. Duan, H. Torosyan, A. K. Doak, K. T. Ziebart, T. Sterling, G. Tumanian, B. K. Shoichet, *J. Med. Chem.* **2015**, *58*, 7076 – 7087.
[13] H. Rao, Z. Li, X. Li, X. Ma, C. Ung, H. Li, X. Liu, Y. Chen, *J. Comput. Chem.* **2010**, *31*, 752 – 763.
[14] S. C. Owen, A. K. Doak, P. Wassam, M. S. Shoichet, B. K. Shoichet, *ACS Chem. Biol.* **2012**, *7*, 1429 – 1435.
[15] A. K. Doak, H. Wille, S. B. Prusiner, B. K. Shoichet, *J. Med. Chem.* **2010**, *53*, 4259 – 4265.
[16] B. Y. Feng, B. H. Toyama, H. Wille, D. W. Colby, S. R. Collins, B. C. H. May, S. B. Prusiner, J. Weissman, B. K. Shoichet, *Nat. Chem. Biol.* **2008**, *4*, 197 – 199.
[17] C. K. McLaughlin, D. Duan, A. N. Ganesh, H. Torosyan, B. K. Shoichet, M. S. Shoichet, *ACS Chem. Biol.* **2016**, *11*, 992 – 1000.
[18] A. N. Ganesh, C. K. McLaughlin, D. Duan, B. K. Shoichet, M. S. Shoichet, *ACS Appl. Mater. Interfaces* **2017**, *9*, 12195 – 12202.
[19] T. Mashimo, Y. Fukunishi, M. Orita, N. Katayama, S. Fujita, H. Nakamura, *Int. J. High Throughput Screening* **2010**, *1*, 99 – 107.
[20] D. Duan, H. Torosyan, D. Elnatan, C. K. McLaughlin, J. Logie, M. S. Shoichet, D. A. Agard, B. K. Shoichet, *ACS Chem. Biol.* **2017**, *12*, 282 – 290.
[21] K. E. D. Coan, B. K. Shoichet, *J. Am. Chem. Soc.* **2008**, *130*, 9606 – 9612.
[22] D. Duan, H. Torosyan, D. Elnatan, C. K. McLaughlin, J. Logie, M. S. Shoichet, D. A. Agard, B. K. Shoichet, *ACS Chem. Biol.* **2017**, *12*, 282 – 290.

Manuscript received: October 18, 2017
Accepted manuscript online: October 23, 2017
Version of record online: November 24, 2017